Free Radical Biology and Medicine 212 (2024) 295–308

Contents lists available at ScienceDirect

Free Radical Biology and Medicine

journal homepage: www.elsevier.com/locate/freeradbiomed

Nitric oxide-induced endoplasmic reticulum stress of *Schistosoma japonicum* inhibits the worm development in rats

Mei Peng [a,b,c,d], Siyu Zhao [a,b,c], Yunyi Hu [a,b,c], Lichao Zhang [a,b,c], Tao Zhou [a,b,c], Mingrou Wu [a,b,c], Meiyining Xu [a,b,c], Kefeng Jiang [a,b,c], Yun Huang [a,b,c], Dinghao Li [a,b,c], Zhao-Rong Lun [b,e], Zhongdao Wu [a,b,c], Jia Shen [a,b,c,*]

[a] Department of Parasitology, Zhongshan School of Medicine, Sun Yat-Sen University, Guangzhou, 510080, China
[b] Key Laboratory of Tropical Disease Control of the Ministry of Education, Sun Yat-Sen University, Guangzhou, 510080, China
[c] Provincial Engineering Technology Research Center for Biological Vector Control, Guangzhou, 510080, China
[d] Department of Laboratory Medicine, The Eighth Affiliated Hospital, Sun Yat-Sen University, Shenzhen, 518000, China
[e] State Key Laboratory of Biocontrol, School of Life Sciences, Sun Yat-Sen University, Guangzhou, 510275, China

ARTICLE INFO

Keywords:
Schistosoma japonicum
Rat
Nitric oxide
Endoplasmic reticulum stress
Development

ABSTRACT

Schistosomiasis, caused by *Schistosoma* spp., is a zoonotic parasitic disease affecting human health. *Rattus norvegicus* (rats) are a non-permissive host of *Schistosoma*, in which the worms cannot mature and cause typical egg granuloma. We previously demonstrated that inherent high levels of nitric oxide (NO), produced by inducible NO synthase (iNOS), is a key molecule in blocking the development of *S. japonicum* in rats. To further explore the mechanism of NO inhibiting *S. japonicum* development in rats, we performed S-nitrosocysteine proteomics of *S. japonicum* collected from infected rats and mice. The results suggested that *S. japonicum* in rats may have undergone endoplasmic reticulum (ER) stress. Interestingly, we found that the ER of *S. japonicum* in rats showed marked damage, while the ER of the worm in iNOS$^{-/-}$ rats and mice were relatively normal. Moreover, the expression of ER stress markers in *S. japonicum* from WT rats was significantly increased, compared with *S. japonicum* from iNOS$^{-/-}$ rats and mice. Using the NO donor sodium nitroprusside in vitro, we demonstrated that NO could induce ER stress in *S. japonicum* in a dose-dependent manner, and the NO-induced ER stress in *S. japonicum* could be inhibited by ER stress inhibitor 4-Phenyl butyric acid. We further verified that inhibiting ER stress of *S. japonicum* in rats promoted parasite development and survival. Furthermore, we demonstrated that NO-induced ER stress of *S. japonicum* was related to the efflux of Ca^{2+} from ER and the impairment of mitochondrial function. Collectively, these findings show that high levels of NO in rats could induce ER stress in *S. japonicum* by promoting the efflux of Ca^{2+} from ER and damaging the mitochondrial function, which block the worm development. Thus, this study further clarifies the mechanism of anti-schistosome in rats and provides potential strategies for drug development against schistosomiasis and other parasitosis.

1. Introduction

Schistosomiasis, caused by *Schistosoma* infection, has been a threat to human health for many years and remains a major public health problem. Estimates show that almost 240 million people required preventive treatment for schistosomiasis in 2019 [1]. There are three major pathogenic species to humans, *Schistosoma mansoni* (*S. mansoni*), *S. japonicum* and *S. haematobium* [2]. The prevalent specie in China is *S. japonicum*. *S. japonicum* is zoonotic species and has more than 40 mammalian species that serve as reservoir hosts [3]. In a permissive host, *S. japonicum* can develop into mature adult worms and lay viable eggs, which is the major cause of schistosomiasis. While some rodent animals, such as *Rattus norvegicus* (rats) and *Microtus fortis*, show natural resistance to *S. japonicum* [4–6]. When *Schistosoma* spp. infect these animals, the worms cannot mature and lay viable eggs and do not cause typical egg granuloma. These animals are referred to as non-permissive hosts of *Schistosoma*. Exploring the mechanism of natural resistance to *Schistosoma* infection in rats can not only elucidate the specific host-parasite interactions but also provide a theoretical basis for establishing new strategies for schistosomiasis prevention and treatment.

* Corresponding author. Department of Parasitology, Zhongshan School of Medicine, Sun Yat-Sen University, Guangzhou, 510080, China.
E-mail address: shenj29@mail.sysu.edu.cn (J. Shen).

https://doi.org/10.1016/j.freeradbiomed.2023.12.032
Received 16 September 2023; Received in revised form 12 December 2023; Accepted 20 December 2023
Available online 21 December 2023

Nitric oxide (NO) is a gas molecule with multiple effects, such as regulating the anti-microbial effect, vascular smooth muscle relaxation, neurotransmission, platelet aggregation, signal transduction, etc. [7,8]. In mammals, NO is produced from L-arginine by three isoforms of NO synthase (NOS), namely, inducible NOS (iNOS), neuronal NOS (nNOS), and endothelial NOS (eNOS) [9]. When stimulated by exogenous factors, such as pathogens infection, large amounts of NO are produced dependent on iNOS [10]. In previous studies, using iNOS knockout ($iNOS^{-/-}$) rats, we have demonstrated that NO, inherently high levels in rats, is an important factor in inhibiting the development of *S. japonicum* in rats [11]. Remarkably, NO inhibited the development of the reproductive organ, which led to a significant decrease in the production of sperms and fertilized eggs and reduced the egg granuloma formation in the liver of rats. We further confirmed that the inhibitory effect of NO was related to the inhibition of mitochondrial oxidative respiration in *S. japonicum* [11]. S-nitrosylation is a reversible post-translational modification, referring to the covalent link of a nitroso group (-NO) with the protein cysteine thiol to form S- nitrosylation [12]. Protein S-nitrosylation is a significant route for NO to exert its ubiquitous biological functions [12,13].

The endoplasmic reticulum (ER) is the closest organelle to mitochondria, which participates in many processes in cells, including protein synthesis, protein fold, protein process, lipid synthesis, carbohydrate metabolism, and calcium (Ca^{2+}) homeostasis [14]. Many factors influence ER homeostasis and induce ER stress, such as parasitic infection [15], oxide [16], and tumor [17]. ER stress, induced by the accumulation of misfolded or unfolded protein in ER lumen or excess release of Ca^{2+} in response to various physiological or pathological factors [18,19], could result in a series of signaling and transcriptional events, collectively known as the unfolded protein response (UPR) [20]. UPR involves reducing the transcription of protein genes, inducing the expression of ER chaperone molecules and degradation-related proteins, thereby reducing the load of unfolded or misfolded protein in the ER lumen, which attempts to restore ER homeostasis [20]. The ER chaperone, glucose-regulated proteins 78 (GRP78), also referred to as immunoglobulin heavy chain binding protein (BiP), plays a key role in the process of UPR [21]. When ER stress happens, the expression of GRP78 significantly increases, and the GRP78 binds unfolded or misfolded proteins and prevents the aggregation of unfolded and misfolded proteins to maintain ER homeostasis [22,23]. Thus, GRP78 is considered a marker of ER stress [22,24]. In addition, glucose-regulated protein 94 (GRP94, also known as Gp96) is also an ER chaperone that assists in protein folding, and the expression of GRP94 also increases in ER stress [25–27]. However, prolonged overloaded ER stress could lead to cell death by activating various death effectors such as BAK, and caspase-12 [28]. Previous studies have shown that NO disrupted ER function and activated ER stress in macrophage and pancreatic β cells, which further induced apoptosis [29,30]. In the study of parasites, it has been reported that NO was able to induce ER stress in *Entamoeba histolytica* [31]. However, no studies have shown whether NO can induce ER stress in schistosomes. In addition, it is unclear whether the inhibition of schistosome development in rats is related to the impairment of schistosome ER function. On the other hand, ER contacted with mitochondria were recognized several decades ago, and their functions were closely linked, including lipid transfer, Ca^{2+} signaling, reactive oxygen species (ROS) signaling, and the transport of proteins and Ca^{2+} from ER to mitochondria to ensure their normal function [32,33]. In our previous study, it is unclear whether the damage to the mitochondrial function of *S. japonicum* in rats is related to the function of ER.

In this study, the S-nitrosylated proteins of *S. japonicum* collected from rats and mice were identified by iodoTMT-based proteomics assay to further explore the mechanism of NO inhibiting the worm development in rats. Using both in vitro culture experiments and in vivo *S. japonicum* infected rat model, we investigated whether the inhibition of NO on the development of *S. japonicum* in rats was related to the ER stress and whether the ER stress of *S. japonicum* affected its mitochondrial function. Elucidation of these issues will provide insight into the mechanisms of anti-schistosome in rats and may provide potential strategies for drug development against schistosomiasis and other parasitosis.

2. Materials and methods

2.1. Ethics approval

All experiments were conducted following the guidelines and with the approval of the Medical Research Ethics Committee of Sun Yat-sen University under license (No. 2018–070).

2.2. Animals

Male BALB/c mice (6–8 weeks) and male SD rats (6–8 weeks) were purchased from the Experimental Animal Center of Guangdong. The $iNOS^{-/-}$ SD strain rats were generated by transcription activator-like effector nucleases (TALENs) technology [11]. All animals were maintained in air-conditioned rooms with a temperature of 22 °C ± 3 °C, 55 % ± 15 % relative humidity, and 12:12 h light/dark photocycle. Animals were fed a commercial diet from Keao Xieli Feed (Beijing, China) and given purified water ad libitum. The *S. japonicum* was collected by cardiac perfusing with phosphate buffer saline (PBS).

2.3. Animal infection and administration

Oncomelania hupensis snails infected with *S. japonicum* were purchased from the Shanghai Institute of Parasitic Diseases (Shanghai, China). All the snails were put in dechlorinated water and placed under a warm lamp for 2 h for cercaria released. After removing the fur on the abdomen, each rat or mouse was percutaneously infected with 200 or 20 cercariae respectively. For in vivo treatment, infected rats received intraperitoneal injections of 4-Phenyl butyric acid (4-PBA, 150 mg/kg/day; Sigma Aldrich, USA). An equal volume of PBS was given to control rats. 5–6 animals per group. The rats were sacrificed at 6 weeks after infection to evaluate *S. japonicum* development and ER stress.

2.4. LC-MS/MS analysis

The worms of *S. japonicum* were collected from infected animals at 6 weeks post-infection. The pretreatment of samples for Mass spectrometric (MS) and MS identification of S-nitrosated cysteine residues was carried out by Shanghai Bioprofile Biotechnology (China). In brief, each sample was ground into powder using liquid nitrogen. All samples, resuspended in lysis buffer, were sonicated for 2 min in the cold water bath. Then proteins were extracted by centrifugation and determined the concentration by the BCA method. Protein (1 mg) from each sample was added by NEM, and the free cysteines of proteins were blocked, and proteins were marked by Biotin-HPDP (Thermo Scientific). And then, the proteins were digested with trypsin. The tryptic digested peptides were first desalted with C18 spin column (Thermo Scientific). The dried peptides were resuspended with 200 μl loading buffer and mixed with 100 μl of high-capacity streptavidin beads (Thermo Scientific) for 1 h at room temperature. The beads were washed and the peptides were labeled with TMT reagents according to the manufacturer's instructions (Thermo Scientific). Washing excess TMT reagents with PBS for many times. And then, all labeled samples were combined equally and washed with PBS once. The mixed labeled peptides were incubated with 200 μl elution buffer for 1 h at room temperature. The eluted peptides were then collected and mixed with 20 mM iodoacetamide to block reduced cysteine residues for 1 h away from light, which indicated the s-nitrosylation sites. Finally, the TMT labeled peptides were fractionated with high-pH reversed-phase using C18 column and six fractions were desalted with C18 StageTips and prepared for further LC-MS/MS analysis.

Liquid chromatography-mass spectrometry (nanoLC-MS/MS) was performed on Nano Flow Rate Easy nLC 1200 chromatography system (Thermo Scientific) for chromatographic separation. The samples were injected and passed through the chromatographic column (75 μm*200 mm, 3 μm, C18, Dr. Maisch GmbH) in buffer A (0.1 % formic acid), and separated with a linear gradient of buffer B (0.1 % (v/v) formic acid, and 85 % (v/v) acetonitrile) at a flow rate of 300 nL/min. The linear gradient was set as follows: 95 % A for column equilibration, 0–2 min, buffer B linear gradient from 2 % to 8 %; 2–45 min, buffer B linear gradient from 8 % to 28 %; 45–50 min, buffer B linear gradient from 28 % to 40 %; 50–52 min, buffer B linear gradient from 40 % to 100 %; 52–60 min, buffer B maintained at 100 %. After the peptide separation, data correlation acquisition (DDA) was performed on a Q-Exactive HF-X mass spectrometer (Thermo Scientific). The analysis duration was 60 min. The parameters for MS1 scanning were set as follows: the scanning range of the parent ion was 350–1800 *m/z*, the resolution was 60,000 (*m/z*: 200), the automatic gain control (AGC) target was 3×10^6, the maximum injection time (IT) was 50 ms. After each full scan, the secondary mass spectrum (MS2 scan) of 20 highest intensity parent ions is triggered to be collected. In the MS2 scan, the resolution was 45,000 (*m/z*: 200), the AGC target was 1×10^5, the maximum IT was 50 ms, the MS2 Activation Type was higher-energy collision dissociation (HCD), the isolation window was set to 1.2 *m/z*, and the normalized collision energy was 32.

2.5. Bioinformatic analysis

The original files were imported into the Proteome Discoverer Software (Version 2.4, Thermo Fisher Scientific, IL, USA) for database retrieval against the database uniprot-*Schistosoma japonicum* (Blood fluke) [6182]-29787-20230,307. fasta, which is sourced from the protein database at https://www.uniprot.org/uniprot/6182. Differentially significant expressed sites were screened with the cutoff of a ratio fold-change of >2 or <0.5 and P-values <0.05. To annotate the sequences, information was extracted from UniProtKB/Swiss-Prot, Kyoto Encyclopedia of Genes and Genomes (KEGG), and Gene Ontology (GO). GO terms were grouped into three categories: biological process (BP), molecular function (MF), and cellular component (CC).

2.6. In vitro culture of S. japonicum

The mature worm of *S. japonicum* were collected from infected BALB/c mice and cultured in Roswell Park Memorial Institute (RPMI)-1640 medium (Gibco; Thermo Fisher Scientific, USA) supplemented with 10 % fetal bovine serum (FBS) (Gibco; Thermo Fisher Scientific, USA), 100 IU/ml penicillin and 100 mg/ml streptomycin (Invitrogen; Thermo Fisher Scientific, USA) incubation at 37 °C in 5 % CO_2. As stated in the Ffigure legends, the worms were treated with different reagents, including Sodium nitroprusside (SNP, 1.5 mM, 3 mM, 5 mM; Sigma-Aldrich, USA), 4-PBA (8 mM; Sigma-Aldrich, USA), and 2-APB (20 μM; Sigma-Aldrich, USA). After 6–24 h of incubation, the worms were collected for subsequent testing.

2.7. Worm and egg burdens measurements

The worms were collected from the hepatic portal vein by perfusion. The worms were placed in a Petri dish containing PBS for counting and photographing under a stereomicroscope. The worm length was measured using Image Pro Plus software. For counting egg burdens, liver tissues from the same part of the liver were weighed and soaked in 4 ml 5 % potassium hydroxide (KOH) for digestion overnight at 37 °C. After fixing the volume of egg suspension to 1 ml, 10 μl of the resuspension was taken for egg counting under the microscope. Every sample was repeated 5 times. And then, the number of eggs per gram of liver tissue was calculated.

2.8. Transmission electron microscopy analysis

The part containing the reproductive organ of the worm was cut off using a surgical blade under a stereomicroscope and fixed in 2.5 % glutaraldehyde overnight at 4 °C. Then these samples were fixed with 1 % osmic acid for 1 h and gradient dehydrated, then embedded in araldite. After ultrathin sectioning, the slices were contrasted with 1 % methanolic uranyl acetate and Reynold's solution of lead citrate and examined using an FEI TecnaiT12 transmission electron microscopy (FEI Company, USA).

2.9. Reproductive organ examination

The collected *S. japonicum* were fixed in 4 % paraformaldehyde. After being washed with PBS three times, the worms were stained with acetic acid magenta solution for 1–2 h and destained in 2.5 % acidic ethanol. Following dehydration in 50%–70%-95%-100%–100 % gradient ethanol for 10 min, worms were transparentized in methyl salicylate for 24 h. Finally, the worms were fixed on glass slides for microscopy observation. A light microscope (Leica, Heidelberg, Germany) was used to observe the structure of the reproductive organ of *S. japonicum*. Observation of sperm and germ cells was done using a laser scanning confocal microscopy (Zeiss, LSM780, Germany) with a 488 nm laser and a 470 nm long pass filter under reflection mode.

2.10. Histopathology

The liver tissues collected from the largest lobe of the liver of infected rats were fixed in 4 % paraformaldehyde and embedded in paraffin. Sections were obtained using an ultra-microtome and stained with hematoxylin and eosin (H&E) for pathological and egg-granuloma analysis. The slides were photographed using a fully automatic digital slide scanner (Zeiss, Germany). The number of egg-granuloma in the same area was counted by using Image Pro Plus software.

2.11. Immunofluorescence analysis

The collected *S. japonicum* were fixed in 4 % paraformaldehyde and embedded in paraffin. Sections were obtained using an ultra-microtome. The paraffin sections were deparaffinized by baking at 60 °C for 30 min and then dehydrated using xylene and gradient ethanol. After incubating with 3 % H_2O_2 for 10 min, the sections were blocked with 1 % bovine serum albumin (BSA) for 1 h and then incubated with GRP78 (Servicebio, China) and GRP94 (Servicebio, China) antibodies overnight at 4 °C. The sections were then incubated with corresponding secondary antibodies. DAPI was used to stain the nuclei. Between all steps, the sections were washed three times in PBS for 5 min each. The slides were photographed using a laser scanning confocal microscopy (Zeiss, LSM880, Germany). The fluorescence intensity was quantified by Image J software.

2.12. TUNEL staining

The collected *S. japonicum* were fixed in 4 % paraformaldehyde and embedded in paraffin. The paraffin sections were deparaffinized and dehydrated using xylene and ethanol. The sections were treated with proteinase K at 37 °C for 22 min and then treated with 0.1 % Triton for 20 min. The TUNEL staining fluid (Servicebio, China) was mixed according to the manufacturer's instructions and added to the sections at 37 °C for 1 h. DAPI was used to stain the nuclei. Between all steps, the sections were washed three times in PBS for 5 min each. The slides were photographed using a laser scanning confocal microscopy (Zeiss, LSM880, Germany). Positive cells were quantified by Image J software.

2.13. Assay for CcO activity

Mitochondria were isolated from the worms by using Mitochondria Isolation Kit (Sigma-Aldrich, USA) and subsequently detected the cytochrome *c* oxidase (CcO) activity according to the manufacturer's instructions of Cytochrome *c* Oxidase Assay Kit (Sigma-Aldrich, USA). In brief, after zeroing the spectrophotometer by adding 0.95 ml of 1X Assay Buffer to a cuvette, the mitochondrial suspension or enzyme solution was added to the cuvette and mixed. Before detection, 50 μl of Ferrocytochrome c Substrate Solution was added and mixed quickly. The A_{550}/minute should be read immediately, and the activity of the sample was calculated from the A_{550}/minute.

2.14. Detection of Ca^{2+} concentration

The Ca^{2+} concentration was detected using Calcium Assay Kit (Abcam, UK) following the manufacturer's instructions. In brief, after being washed in cold PBS, the worms were resuspended in Calcium Assay Buffer and homogenized with a sonicator. Then the samples were centrifuged for 5 min at a top speed of 4 °C. Following prepared all samples and standards, 50 μl of the samples, 90 μl of the Chromogenic Reagent, and 60 μl of Calcium Assay Buffer were added to 96 well plates. The mixtures were incubated at room temperature for 5–10 min protected from light. The concentration was calculated from the absorbance value, which was measured at 575 nm using a microplate reader (TECAN, Austria).

2.15. Real-time quantitative PCR

The collected worms were placed in 0.5 ml Trizol reagent (Invitrogen, USA) and mashed with a TissueLyser II (Qiagen). Total RNA was isolated and purified with chloroform and isopropanol. Purified RNA was quantified with NanoDrop 2000 (Thermo Scientific, USA). Using the PrimeScript RT reagent kit (Takara, Japan), the total RNA was reversed to cDNA according to the manufacturer's instructions. Real-time PCR for quantitative mRNA expression analyses was performed on a real-time quantitative PCR system (Bio-Rad, USA) using the SYBR R Premix Ex Taq TM (Takara, Japan) in a 20 μl volume. PSMD4 was used as the internal gene, and the 2-ΔΔCt method was used to calculate the relative mRNA expression. PSMD4 primers were as follows: forward 5′-CCTCACCAACAATTTCCACATCT-3′, and reverse 5′-GATCACTTATAGCCTTGCGAACAT-3′. GRP78 primers: forward 5′-GGCACAACATATTCCTGCGT-3′, and reverse 5′- CTGGTTCTTGGCAGCATCTC-3′. GRP94 primers: forward 5′-TCTGTGCTGTCCGATATCCC-3′, and reverse 5′- ATCATGCGGTCAACTTCAGC-3′.

2.16. Statistical analysis

All histograms and statistical analyses were performed using GraphPad Prism 7.0. Significant differences between the two groups were determined using unpaired *t*-test with Welch's correction or one-way ANOVA. All data are shown as mean ± SEM and as a single value. $P < 0.05$ was considered statistically significant.

3. Results

3.1. S-nitrosocysteine proteomics of S. japonicum provides mechanistic insight into the inhibitory effect of NO on worm development in rats

In previous studies, we have confirmed that *S. japonicum* in rats (non-permissive hosts of *S. japonicum*) were exposed to high level of NO, while the worms in mice (permissive host of *S. japonicum*) were not [11]. To further explore the mechanism of NO inhibiting *S. japonicum* development in rats, a S-nitrosocysteine proteomics of *S. japonicum* collected from infected rats and mice was performed. By utilizing the iodoTMT-based proteomisc, a total of 2719 cysteine sites corresponding to 1299 proteins were identified in *S. japonicum*. Compared with mice, the results showed that 2346 reliable S-nitrosylation sites up-regulated and only 1 down-regulated in rats (Fig. 1A). The pathway enrichment analysis showed that most of the significant KEGG pathways were involved in the metabolism pathway, including carbon metabolism, glycolysis, pyruvate metabolism, citrate cycle, etc. (Fig. 1B). The result suggests that NO may disturb the metabolic processes of *S. japonicum* by S-nitrosylation to inhibit the worm development in rats. In addition, gene Ontology (GO) subcellular location were analyzed, and the result showed 13 S-nitrosylated proteins located in the mitochondria and 9 S-nitrosylated proteins located in the endoplasmic reticulum (Fig. 1C). Moreover, the GO functional annotation of cellular component (CC), biological process (BP), and molecular function (MF) were analyzed. As shown in Fig. 1D, some of the upregulated S-nitrosylated proteins in *S. japonicum* collected from rats participated in protein transport, protein fold, protein binding, unfolded protein binding, and protein folding chaperone, which participate in UPR (Fig. 1D). In addition, we found that the S-nitrosylation modification of protein folding chaperones of *S. japonicum* collected from infected rats was significantly higher than that of *S. japonicum* collected from infected mice, such as T-complex protein 1 (TCP-1, cytosolic chaperone helping protein fold) subunit and protein disulfide-isomerase (PDI, the primary catalyst for protein folding) (Fig. 1E). These results suggest that NO may induce UPR of *S. japonicum* in rats.

3.2. NO induces ER stress in S. japonicum from infected rats

To investigate whether UPR (ER stress) is involved in the inhibitory effect of NO on the development of *S. japonicum* in rats, we first employed electron microscopy to analyze the ER morphology of *S. japonicum* collected from mice, WT rats, and $iNOS^{-/-}$ rats. As shown in Fig. 2A and B, the ER of the well-developed *S. japonicum* from mice and $iNOS^{-/-}$ rats were tightly packed in these multi-lamellar structures, with individual layers consisting of a dark stripe of ER lumen delimited by two white lines, which represents the normal ER morphology with a clear structure and orderly arrangement. In contrast, the ER of the stunted *S. japonicum* from WT rats was expanded, swollen, formed large numbers of ring-shaped ER whorls and engulfed by vacuolar membrane (Fig. 2B). The statistical analysis results showed that compared with the ER of *S. japonicum* in mice and $iNOS^{-/-}$ rats, the length of ER of the worms in WT rats was significantly reduced and the number of the ring-shaped ER whorls (abnormal ER) was significantly increased (Fig. 2C and D). That this abnormal ER morphology found in the worms from WT rats was consistent with the ER morphological characteristics of ER stress induced by dithiothreitol [34]. In addition, the mRNA expression of ER stress marker molecules in *S. japonicum* from mice, WT rats and $iNOS^{-/-}$ rats, such as *GRP78* and *GRP94*, was further detected by Q-PCR. In comparison with the *S. japonicum* from mice, the results showed that the expression levels of *GRP78* and *GRP94* in *S. japonicum* from WT rats were significantly increased (Fig. 2E and F), which indicates that ER stress response has occurred in *S. japonicum* from rats. However, when NO was deficiency in $iNOS^{-/-}$ rats, the *GRP78* and *GRP94* expressions in *S. japonicum* were significantly decreased, compared with the poor-developed *S. japonicum* from WT rats (Fig. 2E and F), which suggests that the ER stress of the well-developed worms in $iNOS^{-/-}$ rats are significantly suppressed.

3.3. NO induces ER stress in S. japonicum in a dose-dependent manner in vitro

To further determine whether the ER stress in *S. japonicum* is induced by the high level of NO in WT rats, the different concentrations of sodium nitroprusside (SNP, a NO donator) were incubated with *S. japonicum* in vitro, and the ER stress of the worms was detected. As shown in Fig. 3A and B, compared with the control group (Vehicle), we found that the expressions of *GRP78* and *GRP94* in *S. japonicum*

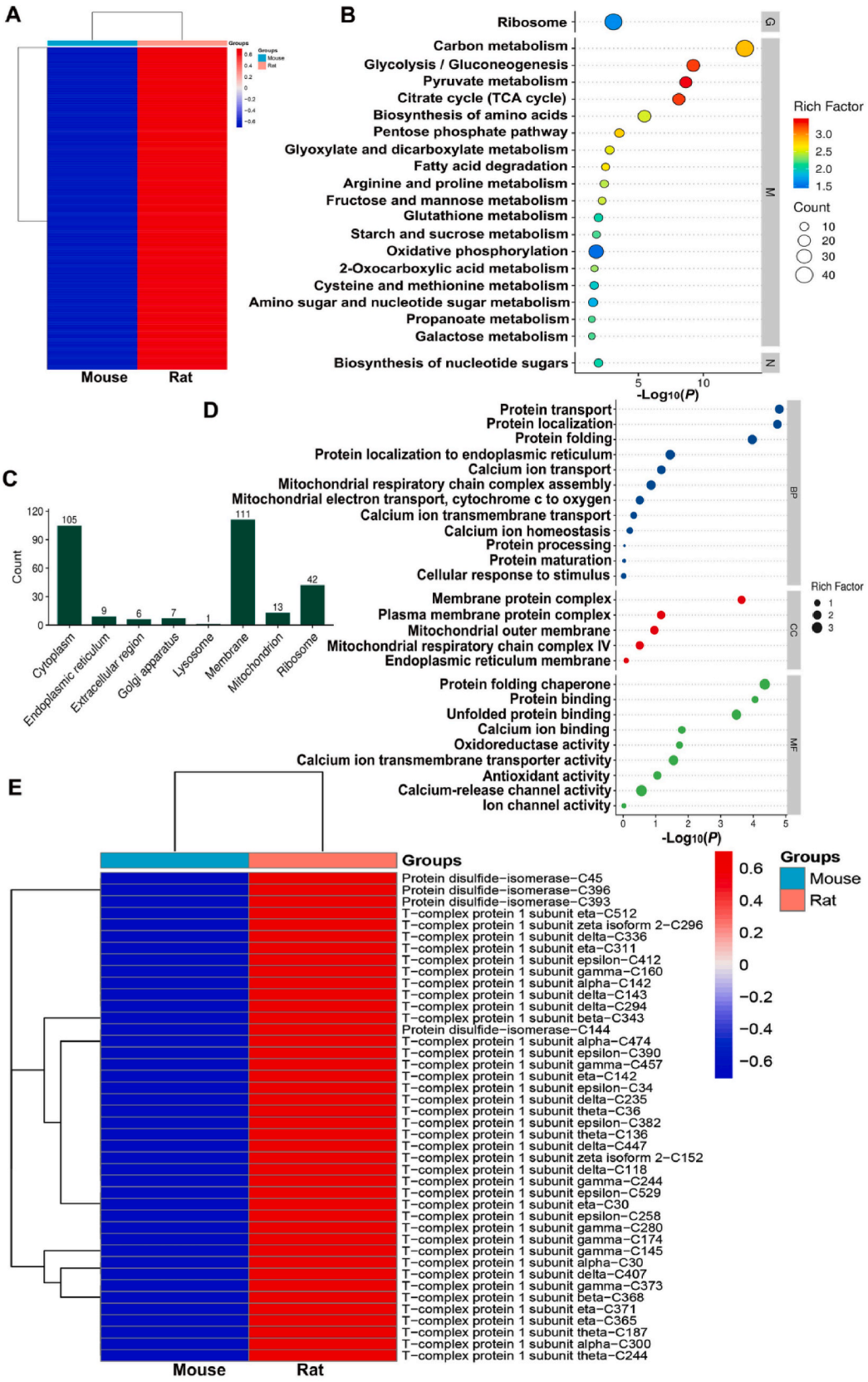

Fig. 1. S-nitrosocysteine proteomics of *S. japonicum* provides mechanistic insight into the inhibitory effect of NO on the worm development in rats. **A** Heatmap showed the 2347 differential S-nitrosylation sites of *S. japonicum* collected from infected rats and mice. **B** Enrichment of the top 20 KEGG pathway by analyzing the differential S-nitrosylated proteins of *S. japonicum* collected from infected rats and mice. **C** GO subcellular location of differential S-nitrosylated proteins of *S. japonicum* collected from infected rats and mice. **D** GO functional classifications by analyzing the differential S-nitrosylated proteins of *S. japonicum* collected from infected rats and mice. **E** Heatmap showed the differential S-nitrosylation sites of protein folding chaperones of *S. japonicum* collected from infected rats and mice. *S. japonicum* were collected from rats and mice at 6 weeks post-infection.

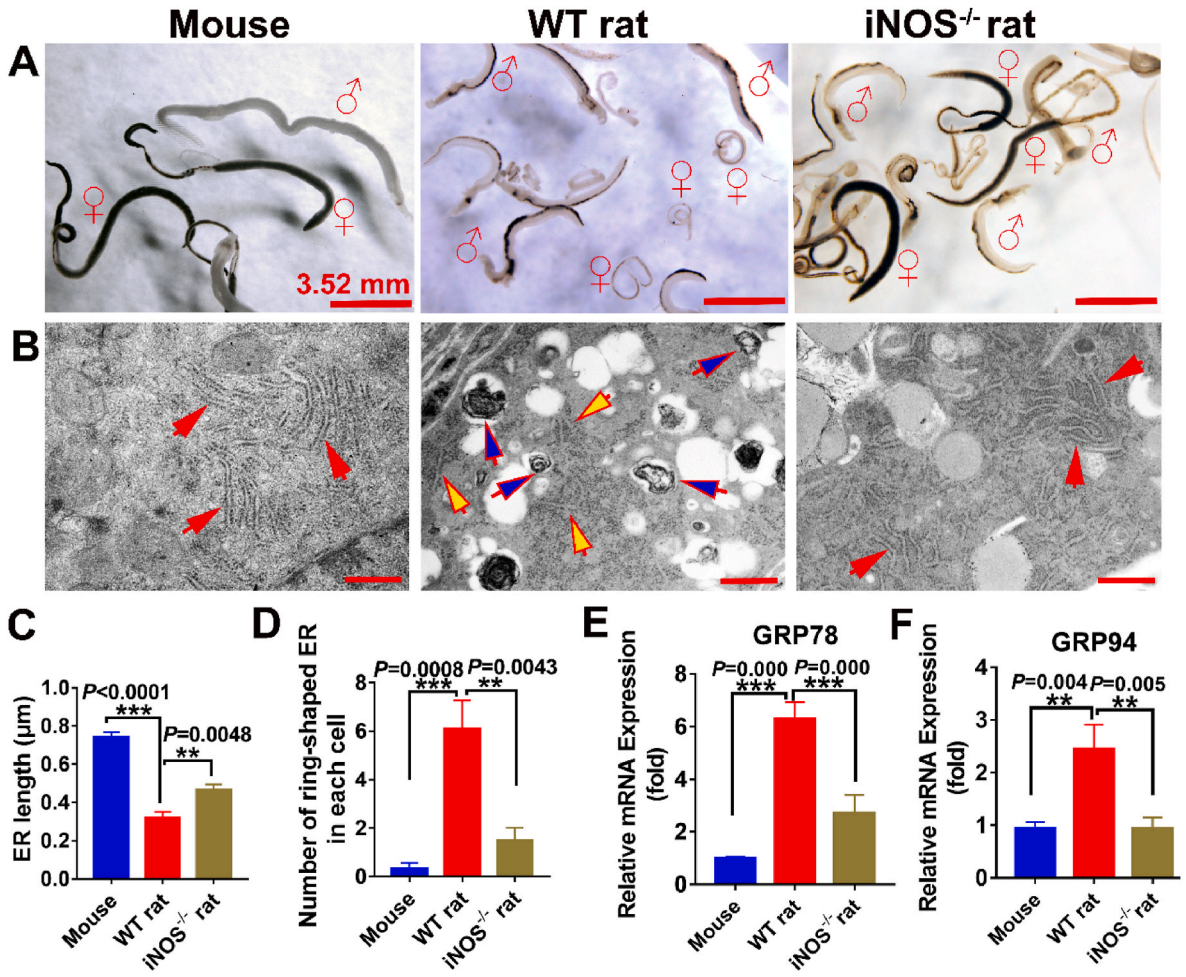

Fig. 2. ER stress occurs in *S. japonicum* from infected WT rats. *S. japonicum* was harvested from infected animals at 6 weeks post-infection. **A** Compared the development of *S. japonicum* in mice, WT rats and iNOS$^{-/-}$ rats by stereomicroscope. ♂, male worms; ♀, female worms. Bars: 3.52 mm. **B** Ultrastructural analysis of the ER morphology in ovarian tissue of adult female *S. japonicum* in mice, WT rats and iNOS$^{-/-}$ rats by transmission electron microscopy. Red arrows indicate normal ER. The ER of *S. japonicum* from WT rats note the expanded and swollen ER (yellow arrows) and the ring-shaped ER whorls inside the vacuole (blue arrows). Bars: 0.5 μm. **C-D** Bar graphs showing the quantification of ER length and number of ring-shaped ER whorls. **E-F** Detecting the mRNA expression of ER stress markers in *S. japonicum* from mice, WT rats and iNOS$^{-/-}$ rats by Q-PCR. Expression was normalized to PSMD4. Data shown are means ± SEM. $^{**}P < 0.01$, $^{***}P < 0.001$.

increased gradually with the rise of the SNP concentration (Fig. 3A and B). When the concentration of SNP was 1.5 mM (low dose, Lo-SNP), the elevated levels of *GRP78* and *GRP94* were not statistically different from the control group ($P > 0.05$). When the SNP concentration was 3 mM (medium dose, Med-SNP) and 5 mM (high dose, Hi-SNP), the *GRP78* and *GRP94* expression levels in *S. japonicum* were significantly higher than that of the control group and increased in a dose-dependent manner (Fig. 3A and B). The results suggest that high concentration of NO can induce ER stress in *S. japonicum*. Furthermore, the results were validated with a commonly known inhibitor of ER stress, 4-Phenyl butyric acid (4-PBA) [35]. Our preliminary experimental results showed that when the concentration of 4-PBA was 8 mM, the parasites did not show obvious toxic reactions (motility and death) and could produce effects, so we chose this concentration for subsequent experiments. Notably, the results showed that the NO-induced ER stress in *S. japonicum* could be inhibited by 4-PBA, as indicated by the lower *GRP78* and *GRP94* levels in *S. japonicum* after being treated with 4-PBA in comparison to the SNP control group (Fig. 3C–H). When ER stress is prolonged and excessive, it can lead to apoptosis (programmed cell death) in damaged cells through a process known as ER stress-induced apoptosis [28]. Therefore, we further investigated the apoptosis induced by NO in *S. japonicum*. The results indicated that NO-induced ER stress could trigger apoptosis in *S. japonicum*, and this phenomenon could be suppressed by the ER stress inhibitor 4-PBA (Fig. 3I and J). These results further demonstrate that NO can induce ER stress in *S. japonicum*.

3.4. Inhibition of ER stress of S. japonicum in rats promotes the parasite development and survival

In order to test whether the ER stress of *S. japonicum* is directly related to the developmental arrest of the worms in rats, we injected the ER stress inhibitor 4-PBA into WT rats to observe the occurrence of ER stress in *S. japonicum* and the worm development. As shown in Fig. 4A, the damage of ER in *S. japonicum* was significantly reduced after treatment with 4-PBA, with evidence that the ER presented a continuous network membrane structure compared with the ER whorls inside the vacuole found in the control group (PBS) (Fig. 4A, B and 4C). In addition, the ER stress inhibitor 4-PBA in rats significantly suppressed the expression of GRP78 and GRP94 in *S. japonicum* and inhibited the occurrence of cell apoptosis (Fig. 4D–I). The results suggest that 4-PBA could effectively inhibit the ER stress of *S. japonicum* in rats. Notably, compared with the control group, the inhibition of the ER stress of *S. japonicum* in rats led to promote the development of the worm with larger sizes (Fig. 4J and K) and significantly increased the worm load (Fig. 4L). In addition, the eggs laid by worm pairs deposited in the liver of rats were significantly increased in the 4-PBA treatment group in

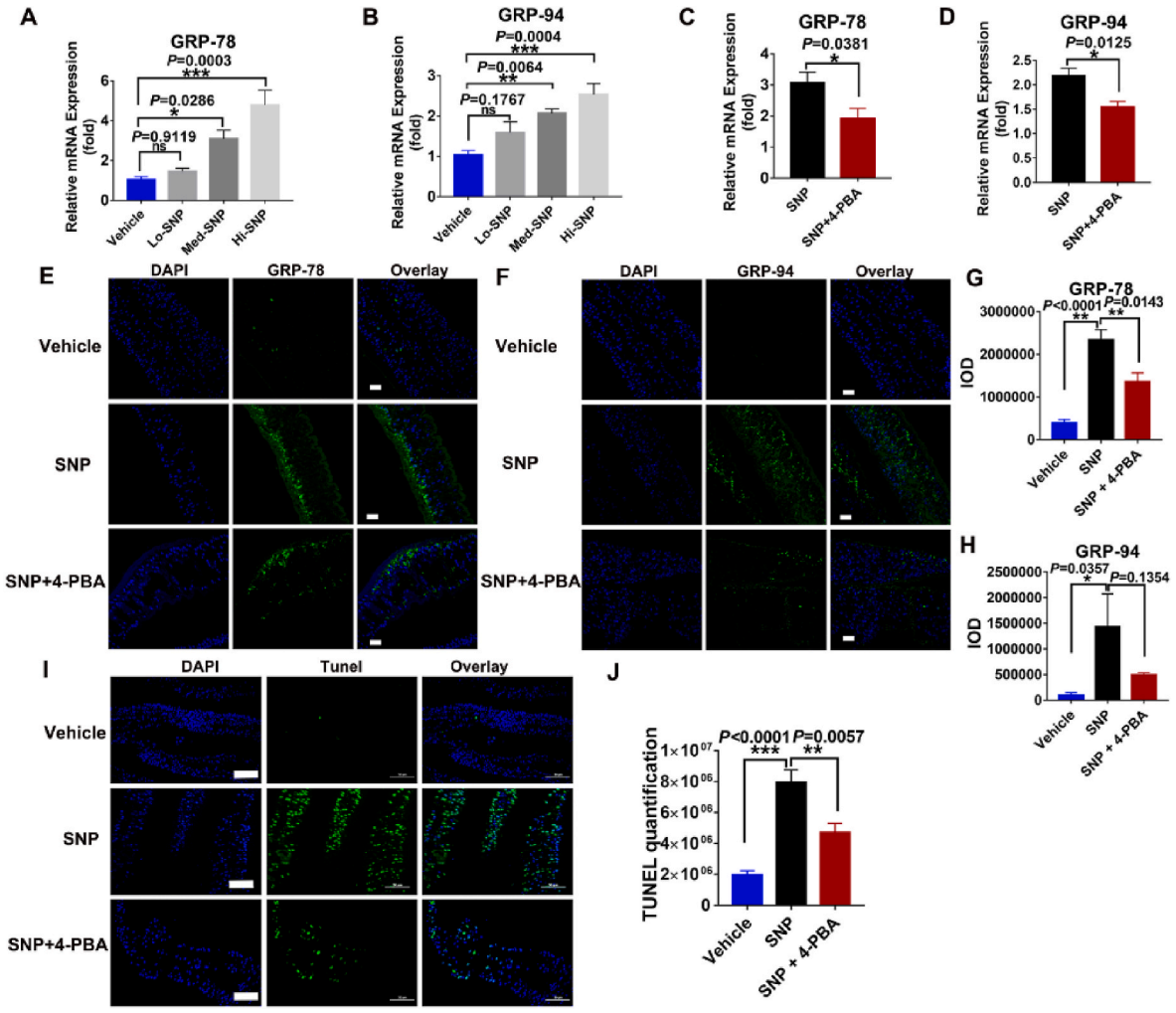

Fig. 3. NO induces ER stress in *S. japonicum* in vitro. **A-B** Q-PCR detected the mRNA expression of ER stress markers in *S. japonicum* after incubation for 12 h with the NO donor SNP at different concentrations. Lo-SNP (1.5 mM), Med-SNP (3 mM), Hi-SNP (5 mM). **C-D** Q-PCR detected the expression of ER stress markers in *S. japonicum* after incubation for 12 h with SNP (3 mM) and 4-PBA (8 mM). 4-PBA: 4-Phenyl butyric acid, an inhibitor of ER stress. Expression was normalized to PSMD4. E-F Immunofluorescence detected the expression of GRP78 and GRP94 in *S. japonicum* after incubation for 12 h with SNP (5 mM) and 4-PBA (8 mM). Scale bar, 20 μm. G-H The expression of GRP78 and GRP94 was quantified by measuring fluorescence intensity. IOD, integrated optical density. I Evaluation of apoptosis by TUNEL staining. Scale bar, 50 μm. J Quantification of TUNEL staining with fluorescence intensity. Data shown are means ± SEM. $^{*}P < 0.05$, $^{**}P < 0.01$, $^{***}P < 0.001$, ns: no statistical significance.

comparison to the control group (Fig. 4M).

Furthermore, when comparing the reproductive systems of male and female *S. japonicum* collected from the control group and the 4-PBA treatment group, we found that the number and size of testicular lobes of the male schistosomes did not show a significant difference between the two groups (Fig. 5A). However, with confocal laser scanning microscopy analysis, we found that the percentage of male worms containing sperm in the seminal vesicles (Control group: 12.92 %; 4-PBA group: 31.58 %) and the number of sperm in the 4-PBA treatment group was significantly higher than that in the control group (Fig. 5A). In the female worms, compared with the control group, the size of ovaries, the percentage of female worms containing eggs (Control group: 4.76 %; 4-PBA group: 23.08 %), and the number of non-excreted eggs in the uterus of *S. japonicum* were significantly increased after 4-PBA treatment (Fig. 5B and C). In addition, the number of egg and egg granulomas in the liver of rats can also reflect the development of the reproductive system of the worms. As shown in Fig. 5D, E and Fig. 4M, rare egg and egg granuloma were found in the liver of rats in the PBS group, while the number of egg and egg granulomas was significantly increased in the 4-PBA treatment group. Collectively, these data strongly suggest that inhibition of ER stress in *S. japonicum* in rats could promote parasite development, increasing egg deposition in the liver and aggravating the pathological damage in rats.

3.5. NO-induced ER stress in *S. japonicum* is related to the efflux of Ca^{2+} from ER

We further explored the mechanism of NO-induced ER stress in *S. japonicum*. The results of S-nitrosocysteine proteomics of *S. japonicum* collected from infected rats and mice showed that the differential S-nitrosylated proteins were involved in calcium ion transport, calcium ion transmembrane transporter activity, calcium ion binding, and calcium ion homeostasis (Fig. 1D). As is well known, ER is an important organelle for Ca^{2+} storage [14]. Therefore, we speculate that NO-induced ER stress could lead to damage to ER, which may result in the release of Ca^{2+} from ER. To test this notion, the level of Ca^{2+} in *S. japonicum* after NO-induced ER stress was detected in vitro. As shown in Fig. 6A, compared with the control group, the level of Ca^{2+} significantly increased after being treated with SNP for 6 and 24 h. However, when the NO-induced ER stress was inhibited by the inhibitor of ER stress 4-PBA, the NO-induced high levels of Ca^{2+} were significantly reduced, especially at 6 h after co-culture (Fig. 6A). These results suggest

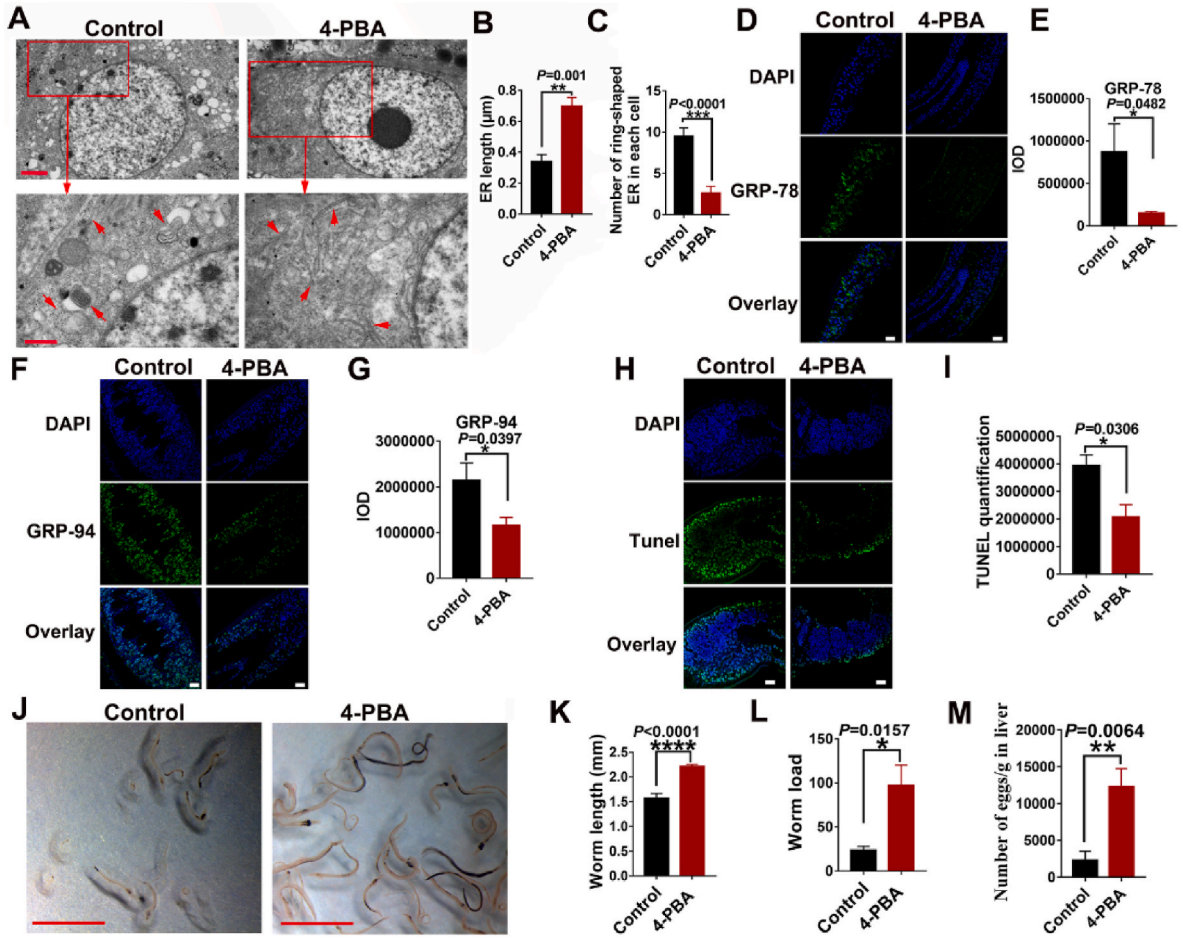

Fig. 4. Inhibition of ER stress in *S. japonicum* in rats promotes parasite development and survival. WT rats were infected percutaneously with 200 *S. japonicum* cercariae and treated with 4-PBA (150 mg/kg/day) or PBS (Control group). Parasites were collected from the portal tract at 6 weeks post-infection. **A**n Ultrastructural analysis of ER morphology in testicular tissue of adult male *S. japonicum*. The red arrow indicates ER. Bar: 1 μm (up) and 0.5 μm (down). **B–C** Bar graphs showing the quantification of ER length and number of ring-shaped ER whorls. **D-G** Immunofluorescence detected the expression of GRP78 (D) and GRP94 (F) in *S. japonicum*. Scale bar, 20 μm. The expression of GRP78 (E) and GRP94 (G) was quantified by measuring fluorescence intensity. **H–I** Evaluation of apoptosis by TUNEL staining in *S. japonicum*. Scale bar, 20 μm. **J** Micrographs of representative parasites from control and 4-PBA-treated rats. Bar: 2 mm. **K** Quantitative analysis of the worm length. **L** Worm load. **M** The number of egg deposition in the liver. Control: infected rats treated with PBS. 4-PBA: infected rats treated with 4-PBA. Data shown are means ± SEM. $^{*}P < 0.05$, $^{**}P < 0.01$, $^{****}P < 0.0001$.

that NO-induced ER stress in *S. japonicum* may be related to the imbalance of Ca^{2+} homeostasis. Furthermore, the Ca^{2+} channel blocker 2-Aminoethoxydiphenyl borate (2-APB, inositol 1,4,5-trisphosphate receptor (IP3R) inhibitor) was used to inhibit the efflux of Ca^{2+} from the ER and maintain the Ca^{2+} concentration in the ER of *S. japonicum*. The result showed that the NO-induced high levels of Ca^{2+} in *S. japonicum* were significantly inhibited by 2-APB (Fig. 6B). Therefore, we further detected the ER stress induced by NO in *S. japonicum* after inhibiting Ca^{2+} efflux from ER by 2-APB. As shown in Fig. 6C and D, the inhibition of the Ca^{2+} channel significantly decreased the expression of *GRP78* and *GRP94* compared with the SNP group (Fig. 6C and D). The results indicate that inhibiting NO-induced Ca^{2+} release can alleviate ER stress and restore ER homeostasis in *S. japonicum*. Thus, these results show that NO-induced ER stress is related to the efflux of Ca^{2+} from ER in *S. japonicum*, which leads to the Ca^{2+} concentration reduction in ER and triggers ER stress in *S. japonicum*.

3.6. NO-induced ER stress in S. japonicum is directly related to the impairment of mitochondrial oxidative respiration

In a previous study, we demonstrated that high levels of NO in rats blocked the development of *S. japonicum* by affecting mitochondrial respiration in the parasite [11]. Here, we also found that the differential S-nitrosylated proteins participated in mitochondrial respiratory chain complex assembly and mitochondrial electron transport, cytochrome *c* to oxygen in the results of S-nitrosocysteine proteomics of *S. japonicum* collected from infected rats and mice (Fig. 1D). And the S-nitrosylation modification of Cytochrome *c* oxidase subunit IV (CcO, the terminal enzyme of the mitochondrial electron transport chain) of *S. japonicum* in rats was increased, compared with the *S. japonicum* in mice (Fig. 7A). These results were consistent with our previous results [11]. In this study, we further investigated whether the impaired mitochondrial function of *S. japonicum* in rats was caused by NO-induced ER stress in the parasite. To verify this hypothesis, the mitochondrial function and mitochondrial morphology of *S. japonicum* were detected after SNP-induced ER stress and inhibition of this ER stress by 4-PBA. The CcO activity of *S. japonicum* was used to assess mitochondrial respiratory function. Compared with the control group, we found that the CcO activity of SNP-treated *S. japonicum* was significantly decreased and partially recovered after inhibited NO-induced ER stress with 4-PBA (Fig. 7B). In addition, the mitochondrial morphology of *S. japonicum* between the SNP group and SNP + 4-PBA group was compared. As shown in Fig. 7C and D, the mitochondria of worms from the SNP group exhibited swelling, cristae disruption, and cristae structure disappeared. However, when the NO-induced ER stress of *S. japonicum* was inhibited by 4-PBA, the mitochondrial exhibited relatively well-defined outer

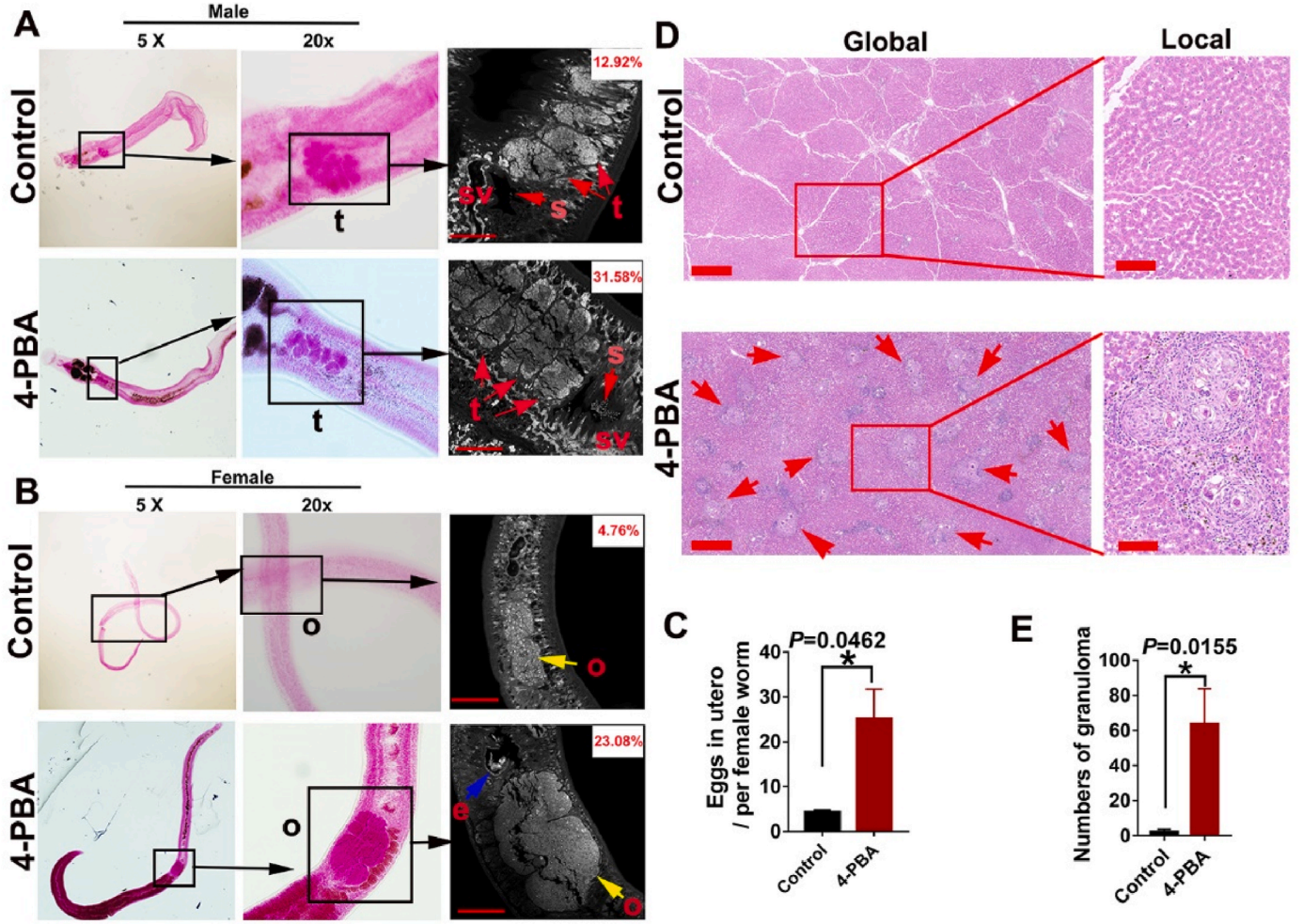

Fig. 5. Inhibition of ER stress in *S. japonicum* in rats promotes reproductive organ development of worm. WT rats were infected percutaneously with 200 *S. japonicum* cercariae and treated with 4-PBA (150 mg/kg/day). Parasites were collected from the portal tract at 6 weeks post-infection. **A-B** Morphological analysis of the reproductive organs' development of male and female worms. The parasites were stained with hydrochloric carmine and observed under a light microscope (Left) and confocal laser scanning microscopy (Right). t, testicular lobules; sv, seminal vesicle; s, sperm; o, ovary; e, egg. The left images were taken at 5× and 20× magnification. In the male worms **(A)**, red arrows indicate sperms, and the values in the upper right corner indicate the percentage of male worms containing sperm. In the female worms **(B)**, yellow arrows indicate ovary, blue arrow indicates egg, and the values in the upper right corner indicate the percentage of female worms containing eggs. Bar: 50 μm. **C** Quantitative analysis of the number of eggs in utero of female worms that contain eggs. **D** Representative H&E staining images of hepatic granulomas. Left (Global) bar: 500 μm; right (Local) bar: 100 μm. Red arrows indicate egg granulomas. **E** Quantitative analysis of the number of egg granulomas in the same area of the liver. Control: infected rats treated with PBS. 4-PBA: infected rats treated with 4-PBA. Data shown are means ± SEM. $^{*}P < 0.05$.

membranes and a clear cristae structure (Fig. 7C and D). Similar results were also found in vivo (Fig. 7E and F). This result suggests that the inhibition of ER stress could reduce the mitochondrial damage in *S. japonicum*.

4. Discussion

In this study, the results of S-nitrosocysteine proteomics of *S. japonicum* suggest that the worms in rats may have undergone UPR (ER stress). With iNOS$^{-/-}$ rat models, our results showed that high levels of NO in rats could induce ER stress in *S. japonicum*. In addition, using the NO donor SNP in vitro, we demonstrated that NO could induce ER stress in *S. japonicum* in a dose-dependent manner, and the NO-induced ER stress in *S. japonicum* could be inhibited by the ER stress inhibitor 4-PBA. Furthermore, 4-PBA also alleviated ER damage of *S. japonicum* in rats. These results demonstrate that inherent high levels of NO in rats can induce ER stress of *S. japonicum*.

NO exerts effects on microorganisms in addition to its direct damage, but also affects biological activities through indirect ways, such as S-nitrosylation [36]. To further explore the mechanism of the effects of NO on *S. japonicum*, a S-nitrosocysteine proteomics of *S. japonicum* collected from infected rats and mice was performed. We found that a higher degree of S-nitrosylation modification occurred in the worms of rats than that of mice. The results of KEGG pathway enrichment analysis showed that the differential S-nitrosylated proteins were predominantly associated with important metabolic processes, including glycolysis, citrate cycle, carbon metabolism, oxidative phosphorylation, etc., which indicates that this posttranslational modification regulated metabolism and mitochondrial bioenergetics in *S. japonicum*. Peng et al. showed that the metabolic formation of several nutrients in *S. japonicum*, namely arginine, proline, glycine, serine, threonine, fatty acids, and vitamin B6, was downregulated in Wistar rats, and they concluded that these may be related to the growth suppression of worms [5]. In addition, glucose metabolism is critical for the survival of schistosomes [37]. Krautz-Peterson et al. showed that suppressing the glucose transporter gene in schistosomes significantly inhibited the viability of the parasites [38]. Therefore, the results suggest that NO may hinder the development of *S. japonicum* in rats by affecting their metabolic process through S-nitrosylation. The GO category showed that these differential S-nitrosylated proteins were related to protein folding, transport,

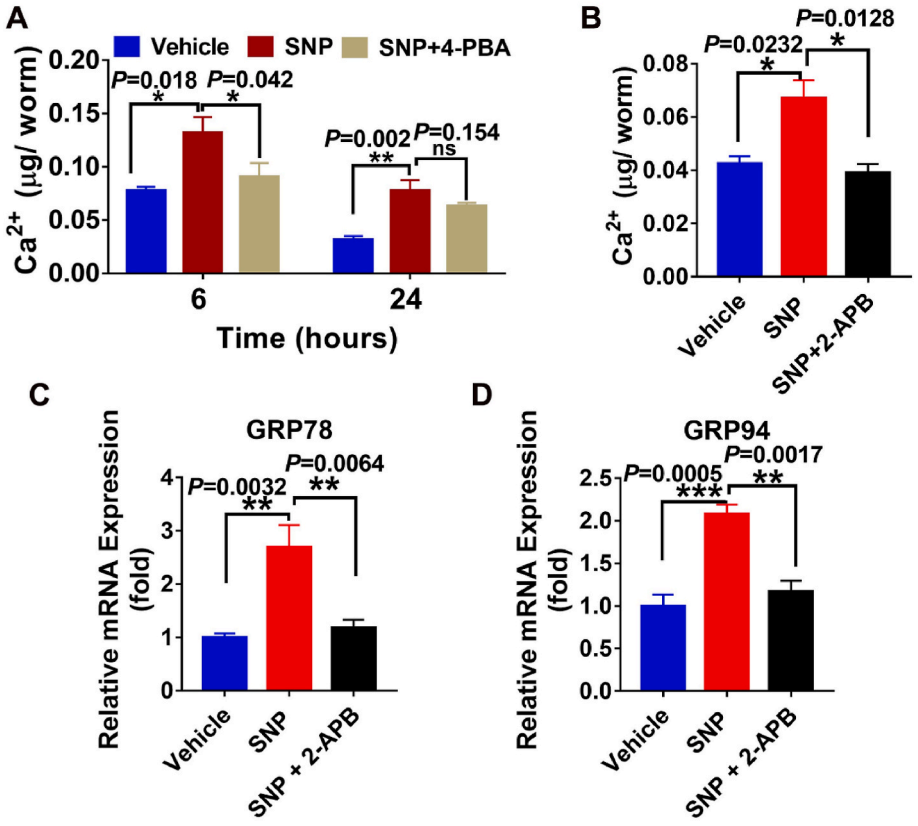

Fig. 6. NO-induced ER stress is related to the efflux of Ca^{2+} from ER. **A** Ca^{2+} concentration of *S. japonicum* after treatment with SNP (3 mM) and 4-PBA (8 mM) for 6 and 24 h. **B** Detecting the level of Ca^{2+} of *S. japonicum* after being treated with SNP and 2-APB. 2-APB: 2-Aminoethoxydiphenyl borate, the IP3R inhibitor. *S. japonicum* was pretreated with 2-APB (20 μM) for 30 min and then SNP (3 mM) was added to the medium. The worms were collected after being co-cultured for 12 h for testing Ca^{2+} concentration. **C-D** Q-PCR detected the expression of ER stress markers in *S. japonicum* after inhibiting Ca^{2+} efflux from ER by 2-APB. *S. japonicum* was pretreated with 2-APB (20 μM) for 30 min and then SNP (3 mM) was added to the medium. The worms were collected after being co-cultured for 12 h. Expression was normalized to PSMD4. Data shown are means ± SEM. $*P < 0.05$, $**P < 0.01$, $***P < 0.001$, ns: no statistical significance.

localization, maturation, and processing, which indicates that the protein folding function of schistosomes in rats may be abnormal. Previous studies have shown that the accumulation of misfolded and unfolded proteins disrupted ER hemostasis and induced ER stress [15]. Consistent with these results, we demonstrated that NO induced ER stress of *S. japonicum* in vivo and in vitro. When UPR occurs, ER chaperones bind to unfolded proteins, to help them refold and prevent them from aggregation, further restoring ER homeostasis [39]. However, in this study, the results of S-nitrosocysteine proteomics revealed that the protein fold chaperones TCP-1 (a cytosolic chaperonin, helps protein fold and is essential for the survival of eukaryotic cells [40]) and PDI (as the primary catalyst for oxidative protein folding, plays an important role in maintaining ER redox homeostasis [41]) showed a significant increase in S-nitrosylation in *S. japonicum* collected from rats, indicating the failure of restoring ER homeostasis. Therefore, these results verify that high levels of NO in rats disturb the protein folding in *S. japonicum* and induce ER stress.

ER stress is implicated in many diseases, including diabetes, neurodegeneration, cancer, etc. [42]. It is reported that ER stress was also involved in female and male reproductive physiopathology in mammals [43–45]. Liu et al. reported that thiamethoxam-induced ER stress disrupted murine ovarian homeostasis and decreased oocyte quality in vitro [44]. Furthermore, Zhang et al. demonstrated that the growth and development of mouse embryos were significantly improved when the induced ER stress response was inhibited [45]. In addition, Kim et al. reported that inhibiting tunicamycin-induced ER stress in *C. elegans* resulted in a significant increase in survivorship, motility, and fecundity [46]. In our study, whether the NO-induced ER stress in *S. japonicum* is related to the inhibition of schistosome development in rats is still unknown. Therefore, the ER stress inhibitor 4-PBA was used to inhibit the ER stress of *S. japonicum* in rats, and the development of the worms was determined. Interestingly, our results showed that the inhibition of ER stress of *S. japonicum* resulted in an increase in worm load, worm length, and the development of reproductive systems of *S. japonicum*, with evidence that the ovary size, the number of eggs in utero, and the number of sperms in seminal vesicle in the 4-PBA treatment group was significantly higher than that in the control group. These results are consistent with previous studies that inhibiting ER stress with 4-PBA alleviated reproductive system damage in mammals [47–49]. Besides, it's well known that excessive ER stress induces apoptosis [28]. Wang et al. showed that more severe apoptosis occurred in *S. japonicum* in rats than in mice, and proposed that differential development of *S. japonicum* in rats and mice may be related to apoptosis [50]. Consistent with this result, we observed a more severe apoptosis in *S. japonicum* in control group than in 4-PBA treatment group. Thus, we speculate that NO-induced ER stress induce apoptosis in worms, which further hinder worm development. Egg granuloma formation in the liver has long been considered as a major cause of morbidity of schistosomiasis [51]. Our results showed that the number of eggs deposited in the liver and hepatic egg granulomas were significantly increased in 4-PBA-treated rats. These results suggest that induction of ER stress in worms may be a potential strategy for drug development against schistosomiasis and other parasitosis.

ER is a multifunctional organelle, mainly participating in protein synthesis, lipid synthesis, Ca^{2+} storage and release [52]. The mechanism of NO-induced ER stress in *S. japonicum* remains unknown. Many factors may disturb ER homeostasis, such as glucose deprivation, aberrant Ca^{2+} regulation, viral infection, environmental toxins, hypoxia, oxidative

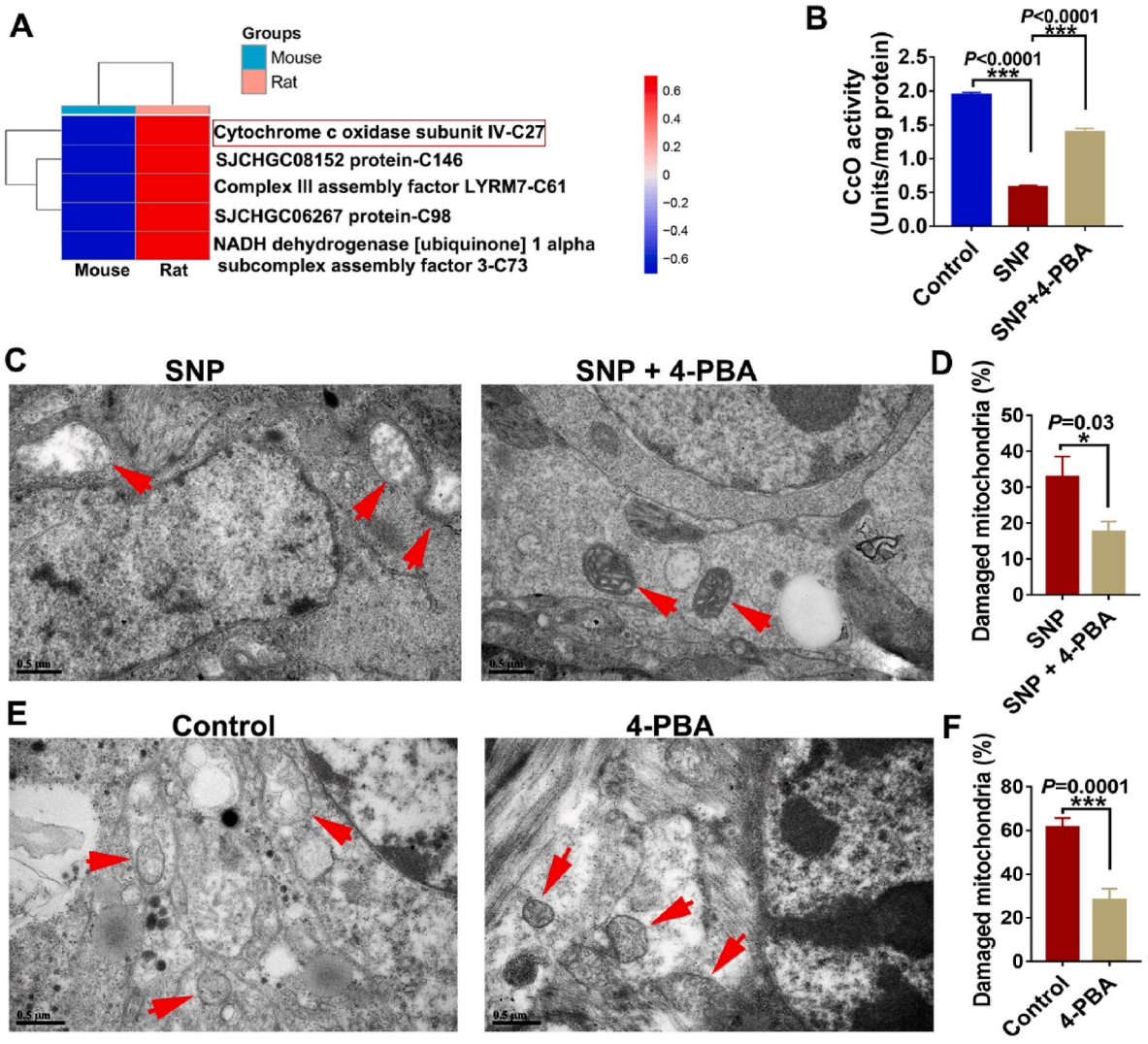

Fig. 7. NO-induced ER stress in *S. japonicum* is related to the impairment of mitochondrial oxidative respiration and mitochondrial damage. **A** Heatmap showed the differential S-nitrosylation sites of mitochondrial respiratory chain complexes of *S. japonicum* collected from infected rats and mice. *S. japonicum* were collected from rats and mice at 6 weeks post-infection. **B** CcO activity from isolated mitochondria of *S. japonicum* after being treated with SNP (3 mM) and 4-PBA (8 mM) for 12 h. **C** Ultrastructural observation of mitochondria in testicular tissue of adult male *S. japonicum* after treatment with SNP (3 mM) and 4-PBA (8 mM) for 24 h. **D** Statistical analysis of the damaged mitochondria from C. **E** Ultrastructural observation of mitochondria in testicular tissue of adult male *S. japonicum* collected from infected WT rats treated with 4-PBA (150 mg/kg/day) or PBS (Control group) at 6 weeks post-infection. Red arrows indicate mitochondria. Bar: 0.5 μm. **F** Quantitative analysis of the damaged mitochondria from E. Data shown are means ± SEM. $^{*}P < 0.05$, $^{**}P < 0.01$, $^{***}P < 0.001$.

injury, hypoglycemia, mutant protein expression, aging, and simple increases in secretory protein synthesis [18]. In this study, the results of S-nitrosocysteine proteomics of *S. japonicum* showed that the proteins involved in “calcium ion homeostasis”, “calcium ion binding” and “calcium ion transport” underwent S-nitrosylated modification in the worms collected from rats. Ca^{2+} homeostasis is closely related to ER homeostasis. The synthesis of some proteins in ER depends on Ca^{2+}, and several ER chaperones and foldases were Ca^{2+}-binding proteins [53]. Therefore, Ca^{2+} homeostasis plays an important role in protein synthesis and maintaining ER homeostasis. Interestingly, we found that NO-induced increased in Ca^{2+} level was decreased by inhibiting ER stress with 4-PBA. Previous studies have shown the interaction between ER stress and Ca^{2+} homeostasis [54,55]. For example, GRP78 and GRP94 participate in maintaining Ca^{2+} homeostasis, and the absence of Ca^{2+} in ER lumen leads to the activation of ER stress and the increase of GRP78 and GRP94 expression [54,55], which is consistent with our study. Two Ca^{2+} channels in ER are responsible for releasing Ca^{2+} into cytosol: IP3Rs and ryanodine receptors (RyRs). It is reported that NO controlled Ca^{2+} homeostasis by affecting IP3Rs and RyRs, such as nitrosylation and phosphorylated IP3R [56]. Xiao et al. showed that palmitic acid (PA) triggered ER-luminal Ca^{2+} release by upregulated IP3R expression and induced ER stress in HepG2 cells [57]. In addition, Oyadomari et al. showed that S-nitroso-N-acetyl-d,L-penicillamine (SNAP, NO donor) induced ER stress by depleting ER Ca^{2+}, which further resulted in pancreatic beta cell apoptosis. Overexpression of calreticulin increased ER Ca^{2+} levels and protected cells against NO-mediated apoptosis [58]. In this study, our results showed that 2-APB (IP3R inhibitor) inhibited the NO-induced increase in Ca^{2+} level and inhibited the expression of GRP78 and GRP94 of *S. japonicum*. In short, the results demonstrate that NO induces ER stress in *S. japonicum* by activating the Ca^{2+} channel and prompting the efflux of Ca^{2+} from ER.

ER and mitochondria are physically connected through mitochondria-associated ER membrane (MAM) [59]. The two organelles are also functionally closely related. Some studies showed that different mitochondrial proteins regulated ER stress [60,61]. The loss of outer mitochondrial membrane GTPase mitofusin 2 (Mfn2) and 54-amino acid microprotein PIGBOS induced ER stress and increased cell death [60,

61]. Biczo et al. demonstrated that mitochondrial dysfunction in the pancreas of mice with acute pancreatitis caused ER stress [62]. On the other hand, the activation of ER stress sensor IRE1 induced mitochondrial damage [63]. Hao et al. showed that the activation of activating transcription factor 4 (ATF4) promoted alcohol-induced hepatic mitochondrial dysfunction [64]. In addition, Xu et al. showed that NO inhibited respiration and changed Ca^{2+} flux between the mitochondria and the ER, which activated ER stress gene GRP78 [65]. Therefore, the relationship between NO-induced ER stress in *S. japonicum* and mitochondrial dysfunction in the worms remains unclear. CcO, complex IV, is the terminal enzyme of the mitochondrial respiratory chain, which accounts for 90 % of cellular oxygen consumption and is required for substantial cellular energy production [66]. Thus, the mitochondrial CcO activity of *S. japonicum* was used to assess mitochondrial respiratory function in this study. Our results showed that NO induced the decrease of CcO activity of *S. japonicum*, which indicates impaired mitochondrial function. Zhang et al. demonstrated that NO-induced persistent inhibition of CcO complex IV was associated with S-nitrosylation of cysteine residues in lung endothelial cells [67]. Consistent with this study, we found that the S-nitrosylation modification of CcO subunit IV of *S. japonicum* collected from infected rats was significantly increased, compared with the *S. japonicum* collected from infected mice. This result showed that NO might impair mitochondrial respiratory function by S-nitrosylation of CcO in *S. japonicum*. We further demonstrated that NO-induced mitochondrial function impairment was alleviated after inhibiting ER stress with 4-PBA in vitro. In addition, when the ER stress of *S. japonicum* in rats was inhibited by 4-PBA, the typical mitochondrial structure was found in *S. japonicum*. Therefore, these results suggest that ER stress is involved in mitochondrial structural and functional damage induced by NO, which further blocks the development of *S. japonicum* in rats.

5. Conclusions

In conclusion, our findings demonstrate that high level of NO could induce ER stress in *S. japonicum*, which participates in blocking the development of *S. japonicum* in rats. Furthermore, we demonstrate that NO-induced ER stress of *S. japonicum* is related to the efflux of Ca^{2+} from ER and the damage to mitochondrial structure and function. It is commonly known that the functions of ER, mitochondria, and Ca^{2+} homeostasis are closely related, but their causal relationship is highly controversial in different conditions and different cells. Thus, this study significantly enhances the understanding of the relationships between NO, ER stress, mitochondrial dysfunction, and Ca^{2+} homeostasis in *S. japonicum*, which further clarifies the mechanism of anti-schistosome in rats and reveals the parasitic features of *S. japonicum* in hosts. These results may provide potential strategies for drug development against schistosomiasis or other parasitosis.

Funding

This work was supported by grants from the National Key Research and Development Program of China (No. 2021YFC2300800, 2021YFC2300801, 2020YFC1200100), the National Natural Science Foundation of China (Grant No. 81802036 and 81871682), the Natural Science Foundation of Guangdong Province of China (2020A1515010896, 2023A1515030050), the Science and Technology Planning Project of Guangdong Province of China (No. 2021B1212040017), the China Postdoctoral Science Foundation (No. 2018M631027 and 2019T120770) and the 111 Project (No. B12003).

Data availability

All data generated or analyzed during this study are included in this published article, the mass spectrometry proteomics data in this paper have been deposited to the ProteomeXchange Consortium with the dataset identifier PXD041667. The login link is https://www.iprox.cn/page/PSV023.html;?url=1682419031418csAJ, the password is UqRE.

CRediT authorship contribution statement

Mei Peng: Data curation, Formal analysis, Investigation, Methodology, Validation, Visualization, Writing – original draft, Writing – review & editing. **Siyu Zhao:** Data curation, Investigation, Methodology, Validation. **Yunyi Hu:** Data curation, Investigation, Methodology, Validation. **Lichao Zhang:** Investigation, Methodology, Validation. **Tao Zhou:** Investigation, Methodology, Validation. **Mingrou Wu:** Investigation, Methodology, Validation. **Meiyining Xu:** Investigation, Methodology, Validation. **Kefeng Jiang:** Investigation, Methodology, Validation. **Yun Huang:** Investigation, Methodology, Validation. **Dinghao Li:** Investigation, Methodology, Validation. **Zhao-Rong Lun:** Resources, Writing – review & editing. **Zhongdao Wu:** Funding acquisition, Resources, Supervision, Writing – review & editing. **Jia Shen:** Conceptualization, Data curation, Formal analysis, Funding acquisition, Investigation, Methodology, Project administration, Resources, Supervision, Validation, Visualization, Writing – original draft, Writing – review & editing.

Declaration of competing interest

None.

Acknowledgments

We would like to thank Yuanjun Guan, Yaqiong Wang, and Juan Li of the Core Lab for Medical Science, Zhongshan School of Medicine, Sun Yat-Sen University for technical assistance.

Abbreviations

NO	nitric oxide
ER	endoplasmic reticulum
WT	wild type
GRP78	glucose-regulated protein 78
GRP94	glucose-regulated protein 94
SNP	sodium nitroprusside
4-PBA	4-Phenyl butyric acid
iNOS	inducible nitric oxide synthase
nNOS	neuronal nitric oxide synthase
eNOS	endothelial nitric oxide synthase
$iNOS^{-/-}$	inducible nitric oxide synthase knockout
Ca^{2+}	calcium
UPR	unfolded protein response
ROS	reactive oxygen species
TCP-1	T-complex protein 1
PDI	protein disulfide-isomerase
Q-PCR	Quantitative real-time PCR
Mfn 2	mitofusin 2
2-APB	2- Aminoethoxydiphenyl borate
CcO	Cytochrome *c* oxidase subunit IV
IP3Rs	inositol 1,4,5-trisphosphate receptors
RyRs	ryanodine recptors
MAM	mitochondria-associated ER membrane
SNAP	S-nitroso-N-acetyl-d,L-penicillamine
IRE1	inositol-requiring enzyme 1
ATF4	activating transcription factor 4
SD rat	Sprague Dawley rat
TALENs	transcription activator-like effector nucleases
SPF	specific-pathogen-free
PBS	phosphate buffer saline
DDA	data correlation acquisition
AGC	automatic gain control

IT	injection time
LC–MS/MS	Liquid chromatography-mass spectrometry
MS	mass spectrometric
HCD	higher-energy collision dissociation
GO	gene Ontology
CC	cellular component
BP	biological process
MF	molecular function
KEGG	Kyoto Encyclopedia of Genes and Genomes
FBS	fetal bovine serum
RPMI	Roswell Park Memorial Institute
KOH	potassium hydroxide
H&E	hematoxylin and eosin

References

[1] WHO, Schistosomiasis, 2022. (Accessed January 6 2022). Available from: https://www.who.int/health-topics/schistosomiasis#tab=tab_1.

[2] D.P. McManus, D.W. Dunne, M. Sacko, J. Utzinger, B.J. Vennervald, X.N. Zhou, Schistosomiasis, nature reviews, Disease primers 4 (1) (2018) 13.

[3] X.N. Zhou, R. Bergquist, L. Leonardo, G.J. Yang, K. Yang, M. Sudomo, R. Olveda, *Schistosomiasis japonica* control and research needs, Adv. Parasitol. 72 (2010) 145–178.

[4] Y. Hu, W. Lu, Y. Shen, Y. Xu, Z. Yuan, C. Zhang, J. Wu, Y. Ni, S. Liu, J. Cao, Immune changes of *Schistosoma japonicum* infections in various rodent disease models, Exp. Parasitol. 131 (2) (2012) 180–189.

[5] J. Peng, H. Han, G.N. Gobert, Y. Hong, W. Jiang, X. Wang, Z. Fu, J. Liu, Y. Shi, J. Lin, Differential gene expression in *Schistosoma japonicum* schistosomula from Wistar rats and BALB/c mice, Parasites Vectors 4 (2011) 155.

[6] J. Shen, S. Xiang, M. Peng, Z. Zhou, Z. Wu, Mechanisms of resistance to *Schistosoma japonicum* infection in Microtus fortis, the natural non-permissive host, Front. Microbiol. 11 (2020) 2092.

[7] R.A. Robbins, M.B. Grisham, Nitric oxide, Int. J. Biochem. Cell Biol. 29 (6) (1997) 857–860.

[8] C. Bogdan, Nitric oxide and the immune response, Nat. Immunol. 2 (10) (2001) 907–916.

[9] U. Förstermann, W.C. Sessa, Nitric oxide synthases: regulation and function, Eur. Heart J. 33 (7) (2012) 829–837, 837a-837d.

[10] C. Nathan, Nitric oxide as a secretory product of mammalian cells, Faseb. J. : official publication of the Federation of American Societies for Experimental Biology 6 (12) (1992) 3051–3064.

[11] J. Shen, D.H. Lai, R.A. Wilson, Y.F. Chen, L.F. Wang, Z.L. Yu, M.Y. Li, P. He, G. Hide, X. Sun, T.B. Yang, Z.D. Wu, F.J. Ayala, Z.R. Lun, Nitric oxide blocks the development of the human parasite *Schistosoma japonicum*, Proc. Natl. Acad. Sci. U. S.A. 114 (38) (2017) 10214–10219.

[12] L. Wang, C. Delahunty, J.H. Prieto, S. Rahlfs, E. Jortzik, J.R. Yates, K. Becker, Protein S-nitrosylation in *Plasmodium falciparum*, Antioxidants Redox Signal. 20 (18) (2014) 2923–2935.

[13] D.T. Hess, A. Matsumoto, S.-O. Kim, H.E. Marshall, J.S. Stamler, Protein S-nitrosylation: purview and parameters, Nat. Rev. Mol. Cell Biol. 6 (2) (2005) 150–166.

[14] D.S. Schwarz, M.D. Blower, The endoplasmic reticulum: structure, function and response to cellular signaling, Cell. Mol. Life Sci. : CM 73 (1) (2016) 79–94.

[15] M. Peng, F. Chen, Z. Wu, J. Shen, Endoplasmic reticulum stress, a target for drug design and drug resistance in parasitosis, Front. Microbiol. 12 (2021) 670874.

[16] H. Liu, W. Lai, X. Liu, H. Yang, Y. Fang, L. Tian, K. Li, H. Nie, W. Zhang, Y. Shi, L. Bian, S. Ding, J. Yan, B. Lin, Z. Xi, Exposure to copper oxide nanoparticles triggers oxidative stress and endoplasmic reticulum (ER)-stress induced toxicology and apoptosis in male rat liver and BRL-3A cell, J. Hazard Mater. 401 (2021) 123349.

[17] X. Chen, J.R. Cubillos-Ruiz, Endoplasmic reticulum stress signals in the tumour and its microenvironment, Nat. Rev. Cancer 21 (2) (2021) 71–88.

[18] H.O. Rashid, R.K. Yadav, H.R. Kim, H.J. Chae, ER stress: autophagy induction, inhibition and selection, Autophagy 11 (11) (2015) 1956–1977.

[19] G. Di Conza, P.C. Ho, ER stress responses: an emerging modulator for innate immunity, Cells 9 (3) (2020).

[20] C. Hetz, K. Zhang, R.J. Kaufman, Mechanisms, regulation and functions of the unfolded protein response, Nat. Rev. Mol. Cell Biol. 21 (8) (2020) 421–438.

[21] Y. Qian, M.H. Falahatpisheh, Y. Zheng, K.S. Ramos, E. Tiffany-Castiglioni, Induction of 78 kD glucose-regulated protein (GRP78) expression and redox-regulated transcription factor activity by lead and mercury in C6 rat glioma cells, Neurotox. Res. 3 (6) (2001) 581–589.

[22] A.S. Lee, The ER chaperone and signaling regulator GRP78/BiP as a monitor of endoplasmic reticulum stress, Methods 35 (4) (2005) 373–381.

[23] Y.S. Park, H.L. Kim, S.H. Lee, Y. Zhang, I.B. Kim, Expression of the endoplasmic reticulum stress marker GRP78 in the normal retina and retinal degeneration induced by blue LED stimuli in mice, Cells 10 (5) (2021).

[24] K. Kaira, M. Toyoda, A. Shimizu, K. Mori, M. Shino, K. Sakakura, Y. Takayasu, K. Takahashi, T. Oyama, T. Asao, K. Chikamatsu, Expression of ER stress markers (GRP78/BiP and PERK) in patients with tongue cancer, Neoplasma 63 (4) (2016) 588–594.

[25] Y. Yang, Z. Li, Roles of heat shock protein gp96 in the ER quality control: redundant or unique function? Mol. Cell. 20 (2) (2005) 173–182.

[26] S. Sharma, F. Ahmad, A. Singh, S. Rathaur, Identification of glucose regulated protein94 (GRP94) in filarial parasite S. cervi and its expression under ER stress, Comparative biochemistry and physiology, Part B, Biochemistry & molecular biology 258 (2022) 110683.

[27] H. Wu, S. Zheng, J. Zhang, S. Xu, Z. Miao, Cadmium induces endoplasmic reticulum stress-mediated apoptosis in pig pancreas via the increase of Th1 cells, Toxicology 457 (2021) 152790.

[28] D. Ron, P. Walter, Signal integration in the endoplasmic reticulum unfolded protein response, Nat. Rev. Mol. Cell Biol. 8 (7) (2007) 519–529.

[29] T. Gotoh, M. Mori, Nitric oxide and endoplasmic reticulum stress, Arterioscler. Thromb. Vasc. Biol. 26 (7) (2006) 1439–1446.

[30] T. Gotoh, S. Oyadomari, K. Mori, M. Mori, Nitric oxide-induced apoptosis in RAW 264.7 macrophages is mediated by endoplasmic reticulum stress pathway involving ATF6 and CHOP, J. Biol. Chem. 277 (14) (2002) 12343–12350.

[31] J. Santi-Rocca, S. Smith, C. Weber, E. Pineda, C.C. Hon, E. Saavedra, A. Olivos-García, S. Rousseau, M.A. Dillies, J.Y. Coppée, N. Guillén, Endoplasmic reticulum stress-sensing mechanism is activated in *Entamoeba histolytica* upon treatment with nitric oxide, PLoS One 7 (2) (2012) e31777.

[32] A.A. Rowland, G.K. Voeltz, Endoplasmic reticulum-mitochondria contacts: function of the junction, Nat. Rev. Mol. Cell Biol. 13 (10) (2012) 607–625.

[33] G. Csordás, D. Weaver, G. Hajnóczky, Endoplasmic reticulum-mitochondrial contactology: structure and signaling functions, Trends Cell Biol. 28 (7) (2018) 523–540.

[34] S. Schuck, C.M. Gallagher, P. Walter, ER-phagy mediates selective degradation of endoplasmic reticulum independently of the core autophagy machinery, J. Cell Sci. 127 (Pt 18) (2014) 4078–4088.

[35] H.P. Pao, W.I. Liao, S.E. Tang, S.Y. Wu, K.L. Huang, S.J. Chu, Suppression of endoplasmic reticulum stress by 4-PBA protects against hyperoxia-induced acute lung injury via up-regulating claudin-4 expression, Front. Immunol. 12 (2021) 674316.

[36] K. Haeussler, K. Fritz-Wolf, M. Reichmann, S. Rahlfs, K. Becker, Characterization of *Plasmodium falciparum* 6-phosphogluconate dehydrogenase as an antimalarial drug target, J. Mol. Biol. 430 (21) (2018) 4049–4067.

[37] H. You, R.J. Stephenson, G.N. Gobert, D.P. McManus, Revisiting glucose uptake and metabolism in schistosomes: new molecular insights for improved schistosomiasis therapies, Front. Genet. 5 (2014) 176.

[38] G. Krautz-Peterson, M. Simoes, Z. Faghiri, D. Ndegwa, G. Oliveira, C.B. Shoemaker, P.J. Skelly, Suppressing glucose transporter gene expression in schistosomes impairs parasite feeding and decreases survival in the mammalian host, PLoS Pathog. 6 (6) (2010) e1000932.

[39] Y. Ma, L.M. Hendershot, ER chaperone functions during normal and stress conditions, J. Chem. Neuroanat. 28 (1–2) (2004) 51–65.

[40] T.M. Smith, B.M. Willardson, Mechanistic insights into protein folding by the eukaryotic chaperonin complex CCT, Biochem. Soc. Trans. 50 (5) (2022) 1403–1414.

[41] L. Wang, X. Wang, C.-c. Wang, Protein disulfide-isomerase, a folding catalyst and a redox-regulated chaperone, Free Radic. Biol. Med. 83 (2015) 305–313.

[42] S.A. Oakes, F.R. Papa, The role of endoplasmic reticulum stress in human pathology, Annual review of pathology 10 (2015) 173–194.

[43] E. Guzel, S. Arlier, O. Guzeloglu-Kayisli, M.S. Tabak, T. Ekiz, N. Semerci, K. Larsen, F. Schatz, C.J. Lockwood, U.A. Kayisli, Endoplasmic reticulum stress and homeostasis in reproductive physiology and pathology, Int. J. Mol. Sci. 18 (4) (2017).

[44] Y. Liu, Q.K. He, Z.R. Xu, C.L. Xu, S.C. Zhao, Y.S. Luo, X. Sun, Z.Q. Qi, H.L. Wang, Thiamethoxam exposure induces endoplasmic reticulum stress and affects ovarian function and oocyte development in mice, J. Agric. Food Chem. 69 (6) (2021) 1942–1952.

[45] J.Y. Zhang, Y.F. Diao, H.R. Kim, D.I. Jin, Inhibition of endoplasmic reticulum stress improves mouse embryo development, PLoS One 7 (7) (2012) e40433.

[46] H.M. Kim, C.H. Do, D.H. Lee, Taurine reduces ER stress in C. elegans, J. Biomed. Sci. 17 (Suppl 1) (2010) S26. Suppl 1.

[47] Y. Wu, C. Ma, H. Zhao, Y. Zhou, Z. Chen, L. Wang, Alleviation of endoplasmic reticulum stress protects against cisplatin-induced ovarian damage, Reprod. Biol. Endocrinol. : RB Elektron. 16 (1) (2018) 85.

[48] E.H. Wang, S.Q. Yao, L. Tao, J.Y. Xi, Sodium 4-phenylbutyrate attenuates high-fat diet-induced impaired spermatogenesis, Biomed. Environ. Sci. : BES (Biomed. Environ. Sci.) 31 (12) (2018) 876–882.

[49] C. Wang, S. Zhang, R. Ma, X. Zhang, C. Zhang, B. Li, Q. Niu, J. Chen, T. Xia, P. Li, Q. Zhao, L. Dong, C. Xu, A. Wang, Roles of endoplasmic reticulum stress, apoptosis and autophagy in 2,2',4,4'-tetrabromodiphenyl ether-induced rat ovarian injury, Reproductive toxicology (Elmsford, N. Y. 65 (2016) 187–193.

[50] T. Wang, X. Guo, Y. Hong, H. Han, X. Cao, Y. Han, M. Zhang, M. Wu, Z. Fu, K. Lu, H. Li, Z. Zhao, J. Lin, Comparison of apoptosis between adult worms of *Schistosoma japonicum* from susceptible (BALB/c mice) and less-susceptible (Wistar rats) hosts, Gene 592 (1) (2016) 71–77.

[51] T.A. Wynn, R.W. Thompson, A.W. Cheever, M.M. Mentink-Kane, Immunopathogenesis of schistosomiasis, Immunol. Rev. 201 (2004) 156–167.

[52] I.X. Zhang, M. Raghavan, L.S. Satin, The endoplasmic reticulum and calcium homeostasis in pancreatic beta cells, Endocrinology 161 (2) (2020).

[53] M. Schröder, R.J. Kaufman, The mammalian unfolded protein response, Annu. Rev. Biochem. 74 (2005) 739–789.

[54] D. Prins, M. Michalak, Organellar calcium buffers, Cold Spring Harbor Perspect. Biol. 3 (3) (2011).

[55] J. Krebs, L.B. Agellon, M. Michalak, Ca(2+) homeostasis and endoplasmic reticulum (ER) stress: an integrated view of calcium signaling, Biochem. Biophys. Res. Commun. 460 (1) (2015) 114–121.
[56] E. Clementi, Role of nitric oxide and its intracellular signalling pathways in the control of Ca2+ homeostasis, Biochem. Pharmacol. 55 (6) (1998) 713–718.
[57] W.C. Xiao, J. Zhang, S.L. Chen, Y.J. Shi, F. Xiao, W. An, Alleviation of palmitic acid-induced endoplasmic reticulum stress by augmenter of liver regeneration through IP3R-controlled Ca(2+) release, J. Cell. Physiol. 233 (8) (2018) 6148–6157.
[58] S. Oyadomari, K. Takeda, M. Takiguchi, T. Gotoh, M. Matsumoto, I. Wada, S. Akira, E. Araki, M. Mori, Nitric oxide-induced apoptosis in pancreatic beta cells is mediated by the endoplasmic reticulum stress pathway, Proc. Natl. Acad. Sci. U.S. A. 98 (19) (2001) 10845–10850.
[59] A.E. Rusiñol, Z. Cui, M.H. Chen, J.E. Vance, A unique mitochondria-associated membrane fraction from rat liver has a high capacity for lipid synthesis and contains pre-Golgi secretory proteins including nascent lipoproteins, J. Biol. Chem. 269 (44) (1994) 27494–27502.
[60] G.A. Ngoh, K.N. Papanicolaou, K. Walsh, Loss of mitofusin 2 promotes endoplasmic reticulum stress, J. Biol. Chem. 287 (24) (2012) 20321–20332.
[61] Q. Chu, T.F. Martinez, S.W. Novak, C.J. Donaldson, D. Tan, J.M. Vaughan, T. Chang, J.K. Diedrich, L. Andrade, A. Kim, T. Zhang, U. Manor, A. Saghatelian, Regulation of the ER stress response by a mitochondrial microprotein, Nat. Commun. 10 (1) (2019) 4883.
[62] G. Biczo, E.T. Vegh, N. Shalbueva, O.A. Mareninova, J. Elperin, E. Lotshaw, S. Gretler, A. Lugea, S.R. Malla, D. Dawson, P. Ruchala, J. Whitelegge, S.W. French, L. Wen, S.Z. Husain, F.S. Gorelick, P. Hegyi, Z. Rakonczay Jr., I. Gukovsky, A. S. Gukovskaya, Mitochondrial dysfunction, through impaired autophagy, leads to endoplasmic reticulum stress, deregulated lipid metabolism, and pancreatitis in animal models, Gastroenterology 154 (3) (2018) 689–703.
[63] D.N. Bronner, B.H. Abuaita, X. Chen, K.A. Fitzgerald, G. Nuñez, Y. He, X.M. Yin, M. X. O'Riordan, Endoplasmic reticulum stress activates the inflammasome via NLRP3- and caspase-2-driven mitochondrial damage, Immunity 43 (3) (2015) 451–462.
[64] L. Hao, W. Zhong, H. Dong, W. Guo, X. Sun, W. Zhang, R. Yue, T. Li, A. Griffiths, A. R. Ahmadi, Z. Sun, Z. Song, Z. Zhou, ATF4 activation promotes hepatic mitochondrial dysfunction by repressing NRF1-TFAM signalling in alcoholic steatohepatitis, Gut 70 (10) (2021) 1933–1945.
[65] W. Xu, L. Liu, I.G. Charles, S. Moncada, Nitric oxide induces coupling of mitochondrial signalling with the endoplasmic reticulum stress response, Nat. Cell Biol. 6 (11) (2004) 1129–1134.
[66] W. Xu, I.G. Charles, S. Moncada, Nitric oxide: orchestrating hypoxia regulation through mitochondrial respiration and the endoplasmic reticulum stress response, Cell Res. 15 (1) (2005) 63–65.
[67] J. Zhang, B. Jin, L. Li, E.R. Block, J.M. Patel, Nitric oxide-induced persistent inhibition and nitrosylation of active site cysteine residues of mitochondrial cytochrome-c oxidase in lung endothelial cells, Am. J. Physiol. Cell Physiol. 288 (4) (2005) C840–C849.